GenoMed Connect
ISSN: 3006-9033
2024, Article ID. 2024.0005, Cite as: www.doi.org/10.69709/GenomC.2024.196011

SCIFINITI

Research Article

OPEN ACCESS

# Identification of Prognostic Biomarkers and Tumor Immune Microenvironment about Uveal Melanoma

**Min Ding**[✉,1,2] **Junfeng Shi**[✉,2,3,*] **Yan Sun**[✉,1,*]

1 Eye Center, Affiliated Hospital of Shandong Second Medical University, Weifang 261041, China
2 Clinical Research Center, Affiliated Hospital of Shandong Second Medical University, Weifang 261031, China
3 Department of Endocrinology and Metabolism, Affiliated Hospital of Shandong Second Medical University, 2428 Yuhe Road, Weifang 261031, China

**Article History**

Submitted: August 04, 2024 Accepted: September 20, 2024 Published: September 23, 2024

**Abstract**

Uveal melanoma (UM) is a malignant eye cancer that has a high mortality rate and is notoriously difficult to diagnose clinically. Identifying prognostic biomarkers and evaluating the tumor immune microenvironment for UM in order to improve diagnosis, treatment decisions and even overall survival for patients. The study involved a comprehensive analysis of transcriptome profiling from the TCGA-UVM project, with the aim of identifying biomarkers and exploring the relationship between the tumor immune microenvironment and UM. A total of 32 differentially expressed genes and 25 RNAs associated with the overall survival (OS) of UM patients were identified. The fusion gene *HSPE1-MOB4* was found to have the highest risk ratio, indicating it plays a key role in the survival rate of these individuals. Through similarity analysis of RNAs expression levels in UM, two subtypes were identified, and the survival rate for Type 1 was notably greater compared to Type 2. Using LASSO regression, a risk model was developed to identify five genes as potential biomarkers for the diagnosis and prediction of overall survival (OS) in patients with UM. Additionally, an association between the risk score and the fraction of immune cells in the Tumor Immune Microenvironment (TIME) was proposed. The observations revealed a significant contrast in both immune score and clustering between high-risk and low-risk groups. These findings offer new insights into approaches for immunotherapy and suggest potential therapeutic targets for individual UM patients.

**Keywords:**

uveal melanoma; prognosis; molecular biomarker; tumor immune microenvironment

## 1. Introduction

Uveal melanoma is the most widespread primary malignancy to originate from eyes in adults, considered to be a rare form of cancer, but it is notoriously aggressive and associated with a high rate of metastasis, making it difficult to treat [1–3]. According to clinical data, the historical one-year overall survival rate of 37% and a median overall survival of 7–8 months, portray a bleak prognosis even in the early stages, when the cancer has already metastasized from the primary site [1]. This is mainly attributed to its aggressive metastatic nature, with nearly 50% of patients showing metastases to other organs such as the liver [2–5], thus making treatments like radiation and surgery largely ineffective [2–5]. Hence, it is of utmost importance to pinpoint prognostic biomarkers for UM and devise treatment strategies that offer greater efficacy for individuals afflicted with UM.

The Tumor Immune Microenvironment (TIME) pertains to the immune environment that surrounds tumor tissues. This microenvironment comprises a complex network of diverse immune cells, such as lymphocytes, monocytes, macrophages, and B cells, alongside the cytokines they generate. The immune system is crucial

* **Corresponding Author:**
Junfeng Shi, Department of Endocrinology and Metabolism, Affiliated Hospital of Shandong Second Medical University, 2428 Yuhe Road, Weifang 261031, China, jfshi@sdsmu.edu.cn; Yan Sun, Eye Center, Affiliated Hospital of Shandong Second Medical University, 288 Shengli East Street, Weifang 261041, China, fysunyan@sdsmu.edu.cn

in regulating the growth and progression of tumors and holds a substantial impact on the eventual treatment outcomes. Research has shown that by disrupting the tumor microenvironment, the immune resistance of the tumor can be effectively enhanced, thereby promoting tumor therapy. Therefore, understanding and analyzing the tumor immune microenvironment, as well as elucidating the molecular and cellular mechanisms that regulate it, has become the latest research focus. Despite this, our understanding of the influence that the TIME exerts on UM remains limited.

Recent research efforts have been made to decipher the molecular events in uveal melanoma, enabling new clinical diagnostics and therapeutics to be established [5–7]. For instance, two common activating mutations, GNAQ and GNA11, were identified, enhancing the understanding of disease pathogenesis and providing a basis for rational therapeutic options based on their presence. [2,8,9]. Additionally, through the use of gene expression profile (GEP)-based classification, UM was divided into two distinct molecular classes, implicating potential significance in personalized treatment decisions [10]. Recently, machine learning (ML) has been used to analyze the interactions between tumor genes and proteins to understand disease progression and develop more effective treatment options. The machine learning algorithms that are frequently employed include SVM, KNN, LASSO, and Random Forest. ML algorithms can be used to identify potential biomarkers for UM, predict outcomes, and classify tumors into subgroups for more personalized treatment approaches. This technology may allow for earlier-stage diagnosis and help clinicians design individualized treatments that are based on the specific patient characteristics.

To this end, the current study seeks to identify molecular biomarkers associated with prognosis of uveal melanoma, as well as construct risk models by machine learning to predict patient survival time. Furthermore, we are exploring the enrichment pathways of these RNAs and the relation between gene expressions and the fraction of six immune cells in TIME, in hopes of providing novel insights for the clinical management of UM.

# 2. Material and Method

## 2.1. Data Collection

The transcriptome profiling data for Uveal Melanoma (UM) was obtained from The Cancer Genome Atlas (TCGA-UVM project), comprising 80 UM samples. To ensure accurate comparison, transcriptome data from 187 normal tissue samples were also obtained from the Genotype-Tissue Expression (GTEx) dataset, accessible through the UCSC Xena browser (https://xenabrowser.net/, accessed on 5 March 2023).

Given the difference in the sources of data (TCGA and GTEx), batch effects were a concern, as they could obscure real biological differences between the tumor and control samples. Therefore, the Fragments Per Kilobase of exon per Million mapped fragments (FPKM) normalization method was employed. FPKM corrects for differences in sequencing depth and gene length, providing normalized expression values that are comparable between samples.

In addition to this, "limma" package in R was used to correct for batch effects using an empirical Bayes framework. This method models technical noise (such as sequencing artifacts or platform-specific effects) while preserving biological variability. Finally, to further standardize the data for analysis and comparison, log-transformation was implemented to all gene expression values to reduce the effect of outliers and make the distributions of gene expression across samples more comparable. This combined approach ensured that differences in gene expression between UM and normal tissues were primarily biological and not artifacts introduced by the data collection processes.

## 2.2. Bioinformatic Analysis

The "survival" package in R (version 4.2.2) was used to calculate the hazard ratio of RNAs, which can identify significant genes related to prognosis. This package was also employed in estimating the relationship between survival time and different groups, as well as survival time and significant RNAs in the tumor tissue. Moreover, "ConsensusClusterPlus" package was employed with 1000 iterations and a resampling rate of 80% to categorize these remarkable RNAs into distinct subtypes [11]. Enrichment analyses were conducted for Gene Ontology (GO) and Kyoto Encyclopedia of Genes and Genomes (KEGG)using the "clusterProfiler" package [12]. Additionally, (GSEA) version 4.1.0 was utilized to discover pathways in which genes participate [13].

The 'estimate' package was utilized to compute the immunoScore using the ESTIMATE method (Estimation of STromal and Immune cells in MAlignant Tumor tissues using Expression data) algorithm [14]. Moreover, cell type identification was conducted to estimate the TIME infiltration levels (CIBERSORT, https://cibersort.stanford.edu/) [15].

## 2.3. Statistical Analysis

Statistical analysis was performed using R version 4.2.2. The *t*-test was initially applied to identify the significant

2024, Vol. 1, Article ID. 2024.0005
www.doi.org/10.69709/GenomC.2024.196011

RNAs between normal and tumor samples. Following that, Pearson correlation test was employed to examine the association between the various subtypes and clinical features, such as stage and age. Subsequently, the LASSO (Least Absolute Shrinkage and Selection Operator) regulation was utilized to construct the risk model: risk score = sum of coefficients ×expression levels of RNAs [16]. The Survival curves were generated via the Kaplan–Meier method. Additionally, the receiver operating characteristic (ROC) curves was employed to reflect the model's predictive ability. And finally, the univariable cox regression was utilized to identify the significant RNAs associated with prognosis [17].

# 3. Result

## 3.1. Expression Levels of RNAs in UM and Normal Tissue

The detailed workflow of the present study is shown in Supplementary Figure S1. After gene expression analysis, 32 genes with significant expression levels between normal and tumor tissue were found ($p < 0.01$, Figure 1A). Of these, the expression levels of 20 RNAs were found to be higher in uveal melanoma tissue as compared to their normal counterparts, including *HLA-DRB1*, *PHLDA2*, *PROSER2*, *TOLLIP-AS1*, *FLYWCH2*, *OGDHL*, *TUBB4A*, *AC004925.1*, *RMND5A*, *OTUD1*, *SCFD2*, *RBM15B*, *WWC2-AS2*, *ZMAT3*, *AC112907.2*, *PTPRH*, *MFSD3*, *AC011481.1*, *KCNE4*, *MT1A*. The remaining genes, like *UPP1*, *RAB4B*, *CAMK1*, *IL32*, *FOXP1*, *PHYKPL*, *HSPE1-MOB4*, *ACOX2*, *APIP*, *NUCB2*, *MITD1* and *SPCS2*, were lower in uveal melanoma than normal tissue.

## 3.2. Identification of Significant RNAs Related to Prognosis

Univariate Cox regression revealed that 25 RNAs were found to be significantly correlated with the overall survival (OS) of individuals with uveal melanoma ($p < 0.05$, Supplementary Figure S2). In addition, the forest plot indicated that 15 genes showed low hazard ratios, implying that patients with higher expression levels of these genes had shorter OS ($p < 0.001$, Figure 1B). For example, *FLYWCH2*, *TUBB4A* and *RBM15B* all had lower expression levels, resulting in longer OS ($p < 0.001$, Figure 1B). On the other hand, the remaining RNAs displayed high hazard ratios, with higher expression levels leading to shorter OS, such as *CAMK1*, *PHLDA2*, and *HLA-DRB1* ($p < 0.001$, Figure 1B). Among all the high-risk genes, *HSPE1-MOB4* was found to have the highest hazard ratio, suggesting a possible crucial role in survival rate of uveal melanoma patients. Furthermore, there were some genes with significantly positive correlations, especially between *TUBB4A* and *RBM15B*, as well as *HLA-DRB1* and *IL32*. However, numerous genes exhibited negative correlations, such as *PD-L1* and *RMND5A*, and *RBM15B* and *NUCB2* (Figure 1C).

## 3.3. Relationship between the Survival Time and RNAs Subtype

Similarity analysis of RNAs expression levels, as well as ambiguous clustering measure percentages, indicated that k = 2 was the optimal clustering stability (Figure 2A and Supplementary Figure S3). This resulted in two different subtypes, namely cluster 1 (n = 53) and cluster 2 (n = 27). Interestingly, the survival rate of the former was found to be significantly greater than that of the latter ($p < 0.001$, Figure 2B). Following a comparison of clinical characteristics such as age and stage, notable differences were observed between the two clusters. To begin with, the expression levels of genes including *ZMAT3*, *OGDHL*, *FOXP1*, *TUBB4A*, *RBM15B*, *AC112907.2*, *FLYWCH2*, *TOLLIP−AS1*, *WWC2−AS2*, *APIP*, *RMND5A*, *OTUD1*, *ACOX2*, *AC004925.1* and *KCNE4* were significantly lower in cluster 2 compared to cluster 1. Conversely, the remaining genes exhibited a contrasting result. Furthermore, the T stage values varied remarkably between both clusters (Figure 2C).

## 3.4. Enrichment Analysis about Prognostic RNAs

Subsequently, the prognostic RNAs of two clusters were further evaluated for enrichment analysis. Results of the Gene Ontology (GO) analysis showed that RNAs were preferentially implicated in Biological Process (BP) and Molecular Function (MF) (Figure 3A,B). Enriched pathways related to immune regulation, such as the regulation of mRNA splicing via spliceosome, positive regulation of B cell receptor signaling, and negative regulation of lymphocyte proliferation, suggest an immune-active microenvironment. These processes contribute to a less aggressive tumor profile with better prognosis (Figure 3C). Key genes involved in cluster 1 UVM include *FOXP1* and *TUBB4A*, which are linked to enhanced immune surveillance and anti-tumor immune responses. The cluster 2 phenotype displayed enrichment in pathways such as mRNA processing, regulation of monocyte differentiation, and dendritic cell antigen processing and presentation, suggesting a more immune-suppressive tumor microenvironment. Cellular components like the intermediate filament and endoplasmic reticulum-plasma membrane contact site are more prominent in cluster 2

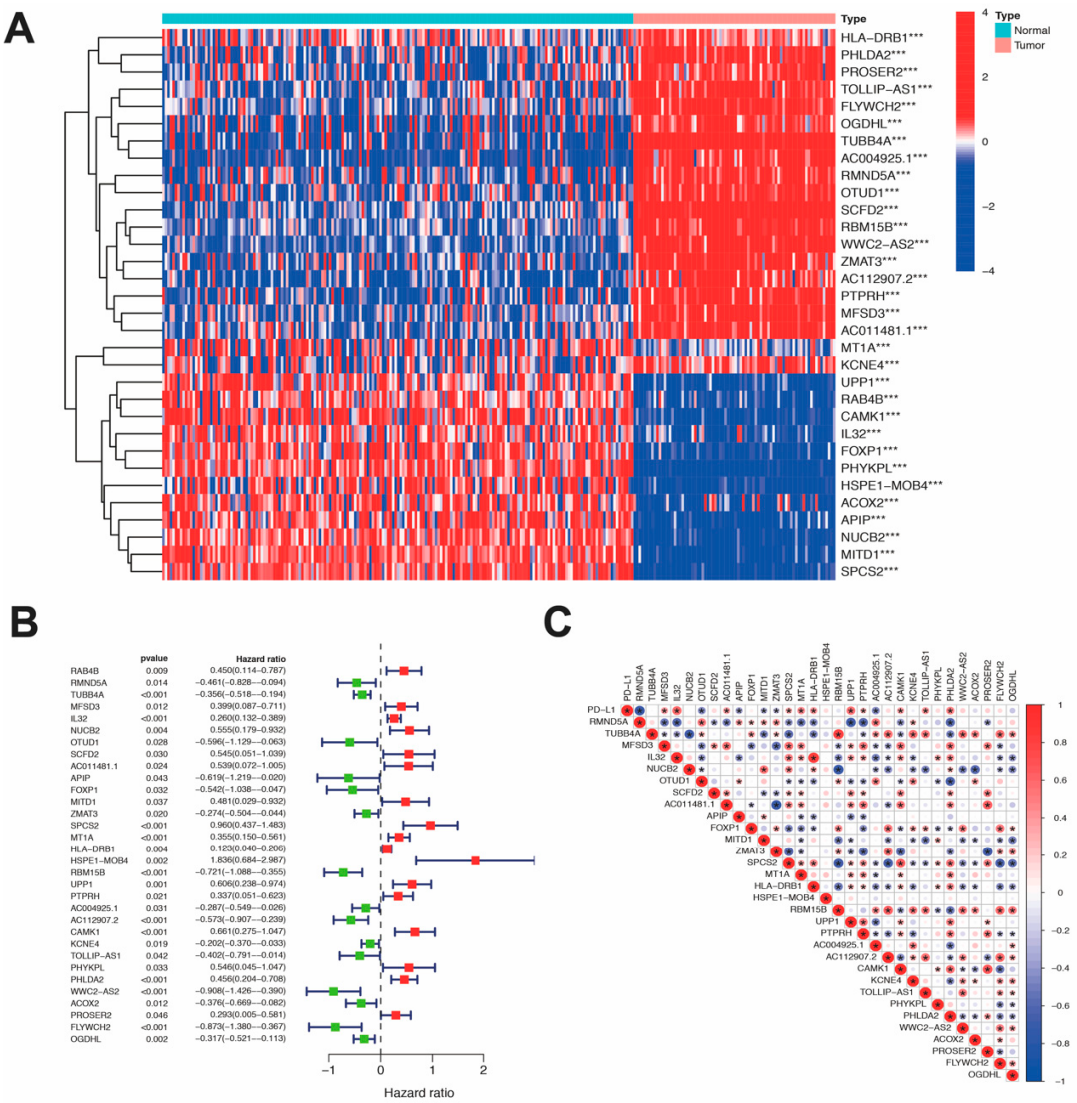


**Figure 1: Expression of genes associated significantly with Uveal melanoma.** (**A**) Genes with significant expression levels between normal tissue and Uveal melanoma. (**B**) Prognostic RNAs related to Uveal melanoma. (**C**) The corrections between prognostic genes. *** $p < 0.001$.

UVM, highlighting a more aggressive and metastatic potential, aligned with poor prognosis. Genes such as *HSPE1*, *CAMK1*, and *HLA-DRB1* contribute to the immune evasion mechanisms and enhance the tumor's ability to progress and resist immune responses. Additionally, the GSEA analysis highlighted that in cluster 2, most genes were involved in pathways such as mTOR (mammalian target of rapamycin) (normalized enrichment score = 1.647, normalized $p$-value < 0.001) and P53 pathway (normalized enrichment score = 1.688, normalized $p$-value = 0.002) (Figure 3D,E).

## 3.5. Construction and Prediction of Risk Model of UM

Using LASSO regression, five RNAs were identified to build a risk model for predicting the overall survival (OS) of patients with uveal melanoma, along with the expression levels of significant RNAs in the UM training cohort (Supplementary Figure S4). This risk model was expressed as follows:

$$\text{risk score} = FOXP1 \times (-0.5664) + HSPE1\text{-}MOB4 \times 2.5721 + CAMK1 \times 0.5360 + WWC2\text{-}AS2 \times (-2.0179) + ACOX2 \times (-0.4066).$$

2024, Vol. 1, Article ID. 2024.0005
www.doi.org/10.69709/GenomC.2024.196011

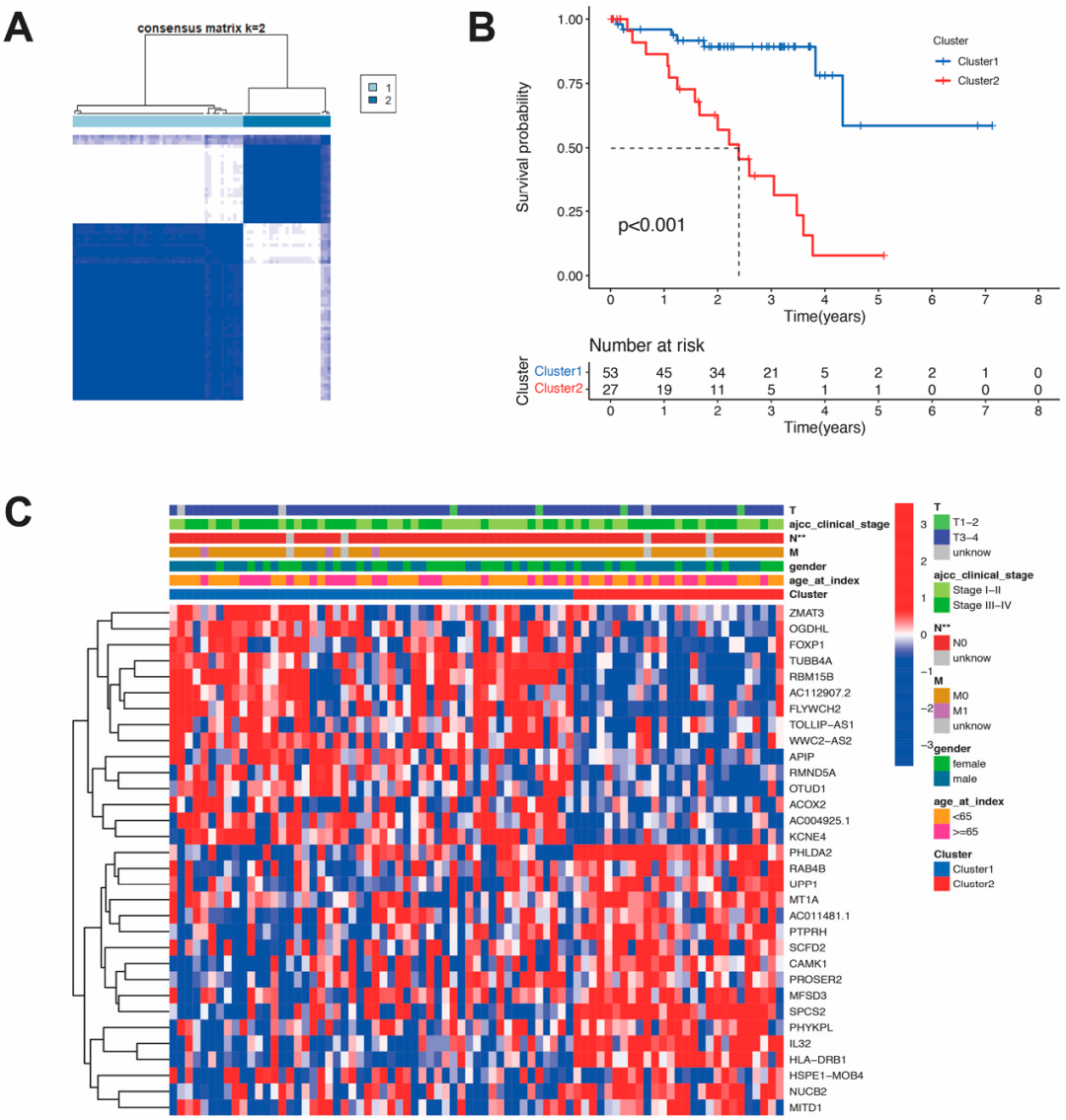


**Figure 2: Differential clinicopathological features and survival of Uveal melanoma in two subtypes.** (**A**) Consensus clustering matrix for k = 2. (**B**) The overall survival (OS) in different subtypes. (**C**) Heatmap and clinicopathologic features of the two clusters (cluster 1/2). ** $p < 0.01$.

2024, Vol. 1, Article ID. 2024.0005
www.doi.org/10.69709/GenomC.2024.196011

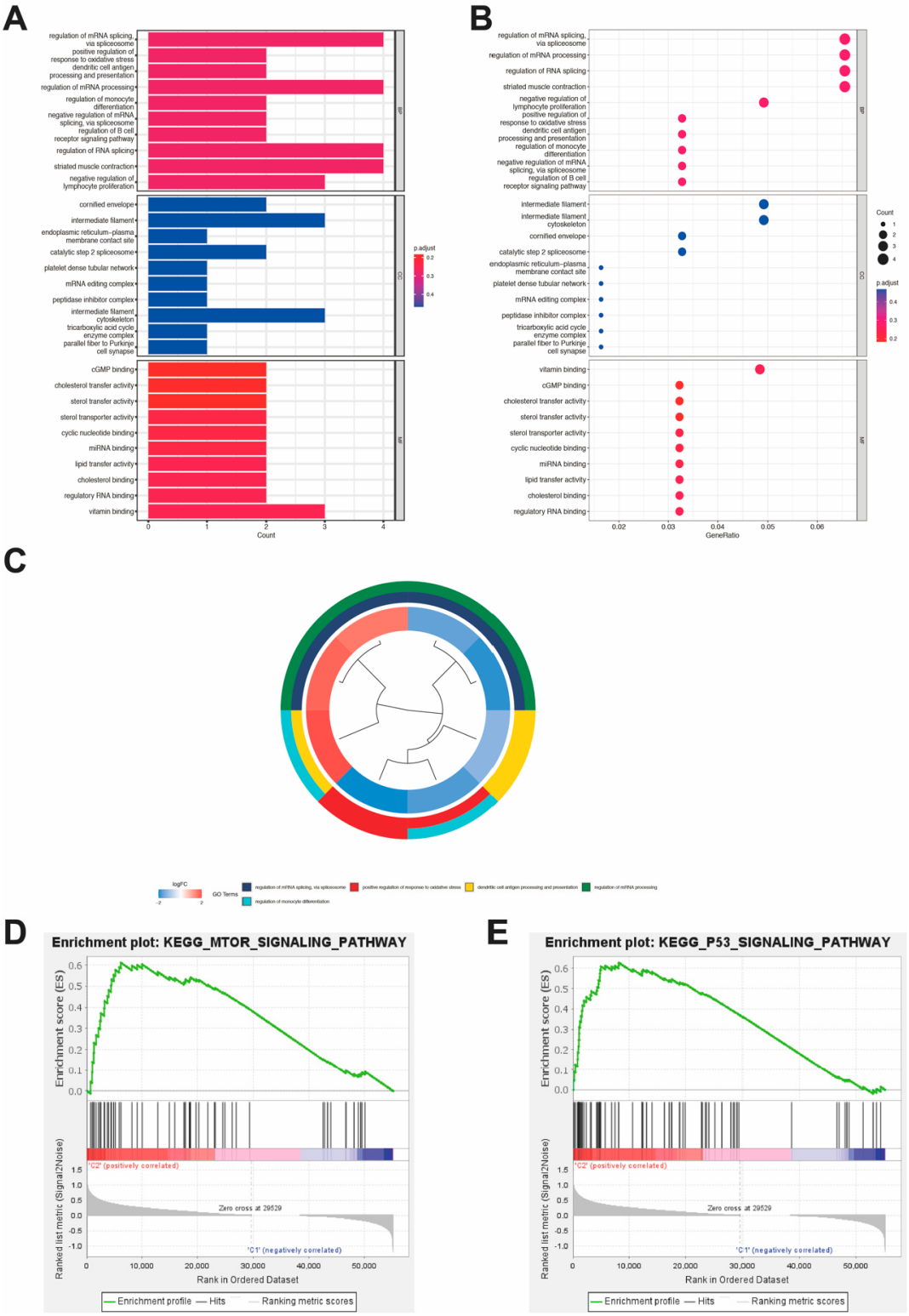


**Figure 3: Enrichment analysis of two clusters.** (**A**–**C**): The enrichment pathway in cluster1 and cluster2 using Gene Ontology (GO) analysis. (**D**,**E**): GSEA analysis in cluster 2.

2024, Vol. 1, Article ID. 2024.0005
www.doi.org/10.69709/GenomC.2024.196011

Based on the median overall risk score, patients with UM were categorized into two groups: high-risk and low-risk groups. The survival rate was significantly greater in low-risk group as compared to high-risk group in both the training and test cohorts ($p < 0.001$, Figure 4A). In test group, we obtained the similar result (Figure 4B).

Additionally, ROC curve analysis was performed to assess the 5 risk features. In training cohort, the Area Under the Curve (AUC) value was 0.92. On the other hand, the AUC value was 0.71 in the test set (Figure 4C,D). This finding supports the effectiveness of the model in accurately predicting the survival rate of patients based on the transcriptome profiling data.

The expression of *HSPE1-MOB4* and *CAMK1* were observed to be significantly increased in the high-risk group, while the expression of *FOXP1*, *WWC2-AS2*, and *ACOX2* were significantly decreased in low-risk group. This was determined by using the risk score to assess the expressions of each gene in both high and low-risk groups (as shown in Figure 4E,F).

### 3.6. Correction between Subtypes and Level of Immune Cell Infiltration in the TIME

The relationships between subtypes and levels of immune cell infiltration in TIME were studied and it was found that there were six significant immune cells in both clusters 1 and 2, including T cells CD8, T cells CD4 memory activated, Monocytes, Macrophages M1, Dendritic cells resting, and Mast cells resting ($p < 0.05$, Supplementary Figure S5). However, only the infiltration of Monocytes was higher in cluster 1 than cluster 2 ($p < 0.001$). In contrast, the remaining five cell types showed lower levels in cluster 1 than cluster 2 (Figure 5A). Moreover, some immune markers such as ImmuneScore of cell fraction, ESTIMATEScore and StromalScore were significantly increased in cluster 2 ($p < 0.001$, Figure 5B–D).

### 3.7. Relation between Clinical Characteries and Risk Score

Moreover, when performing the survival analysis, differences between high and low-risk group were observed in clinical features such as age ($p < 0.001$, Figure 6A,B), gender ($p < 0.002$, Figure 6C,D), M stage ($p < 0.001$, Figure 6E), N stage ($p < 0.001$, Figure 6F) and T stage ($p < 0.001$, Figure 6G). On top of that, Figure 6H illustrated that ImmunoScore and cluster had remarkable dissimilarities in both high and low-risk groups (Supplementary Figure S6).

### 3.8. Risk Score Associated with the Immune Cell Infiltration in the TIME

Furthermore, the relationship among the risk score and six types of immune cells in the tumor immune microenvironment (TIME) of UM was also investigated. The analysis revealed a positive correlation between the risk score and some immune cells, such as dendritic cells resting, macrophages M1, T cells CD4 memory activated, and T cells gamma delta ($p < 0.05$, Figure 7A–D). Conversely, some immune cells fractions had a negative relation to risk score, such as B cells naïve, Monocytes, NK cells activated, Plasma cells ($p < 0.05$, Figure 7E–H).

## 4. Discussion

In the last decades, many studies have showed that expression of RNAs can be used to predict and treat cancer. For instance, a high level of *SChLAP1* expression has been found to be a meaningful biomarker in prostate cancer [18]. Similarly, previous research illustrated that *PUS7* is a potential biomarker for ovarian cancer [19]. Moreover, the expression of some genes has been associated with tumor prognosis, which offers new insights for treatment. For example, RNA levels of *topoisomerase II* $\alpha$ (*TOP2A*) have been identified as a reliable prognostic marker, as well as related to favorable response to anthracycline-based therapy [20]. In this study, the aim was to examine the connections between RNAs and uveal melanoma (UM) in order to explore its molecular pathogenesis. In this research, we proposed that *HSPE1-MOB4* has a significant association with the prognosis of UM, though there is limited research available on this gene. Therefore, future research should focus on investigating the association between the expression of *HSPE1-MOB4* and treatment options.

*HSPE1-MOB4* is a type of fusion transcript, formed by the adjacent genes *HSPE1* and *MOB4* fused together for transcription. It has been reported that this fusion transcript was observed in the analysis of follicular thyroid cancer, but its role in UM remains unclear [21]. The oncogenic fusion gene was initially discovered in malignant hematological tumors, where the chromosome translocations frequently lead to the fusion of two genes, producing abnormal protein products [22,23]. Fusion genes resulting from chromosome translocations are known to produce abnormal protein products and have been recognized as important prognostic indicators and targets for therapy [24]. Heat shock protein family member 1 (*HSPE1*) is a member of the heat shock protein family, which can act as a "chaperone" in conjunction with heat shock protein family D member 1 (*HSPD1*) to facilitate proper protein fold-

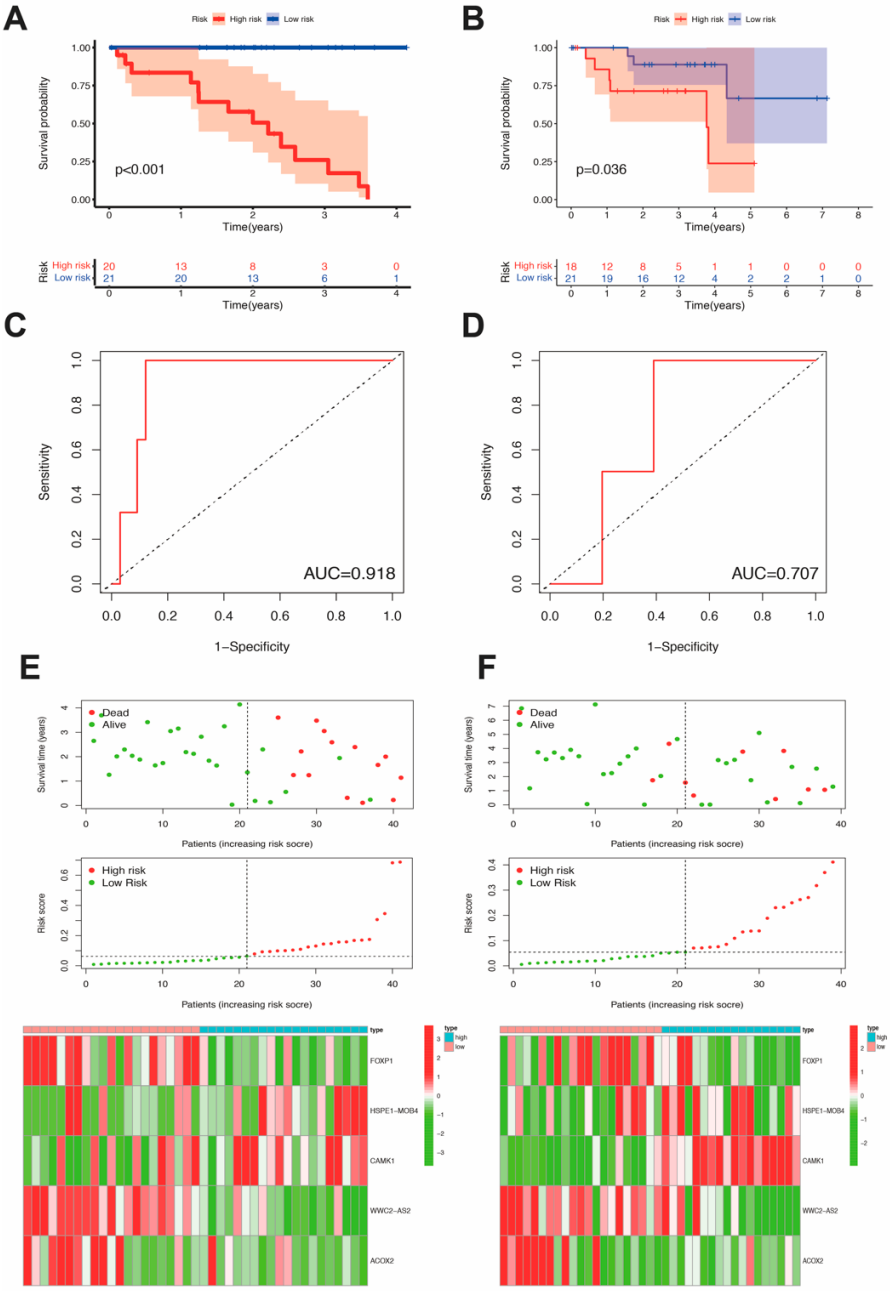


**Figure 4: Comparison of prognosis between high- and low-risk groups.** (**A**) The OS of high- and low-risk in training cohort. (**B**) The OS of high- and low-risk in test set. (**C**) Receiver operating characteristic curve of training set. (**D**) Receiver operating characteristic curve in test cohort. (**E**) Expression levels of 5 prognostic genes in training set. (**F**) Expression levels of 5 RNAs about test cohort.

2024, Vol. 1, Article ID. 2024.0005
www.doi.org/10.69709/GenomC.2024.196011

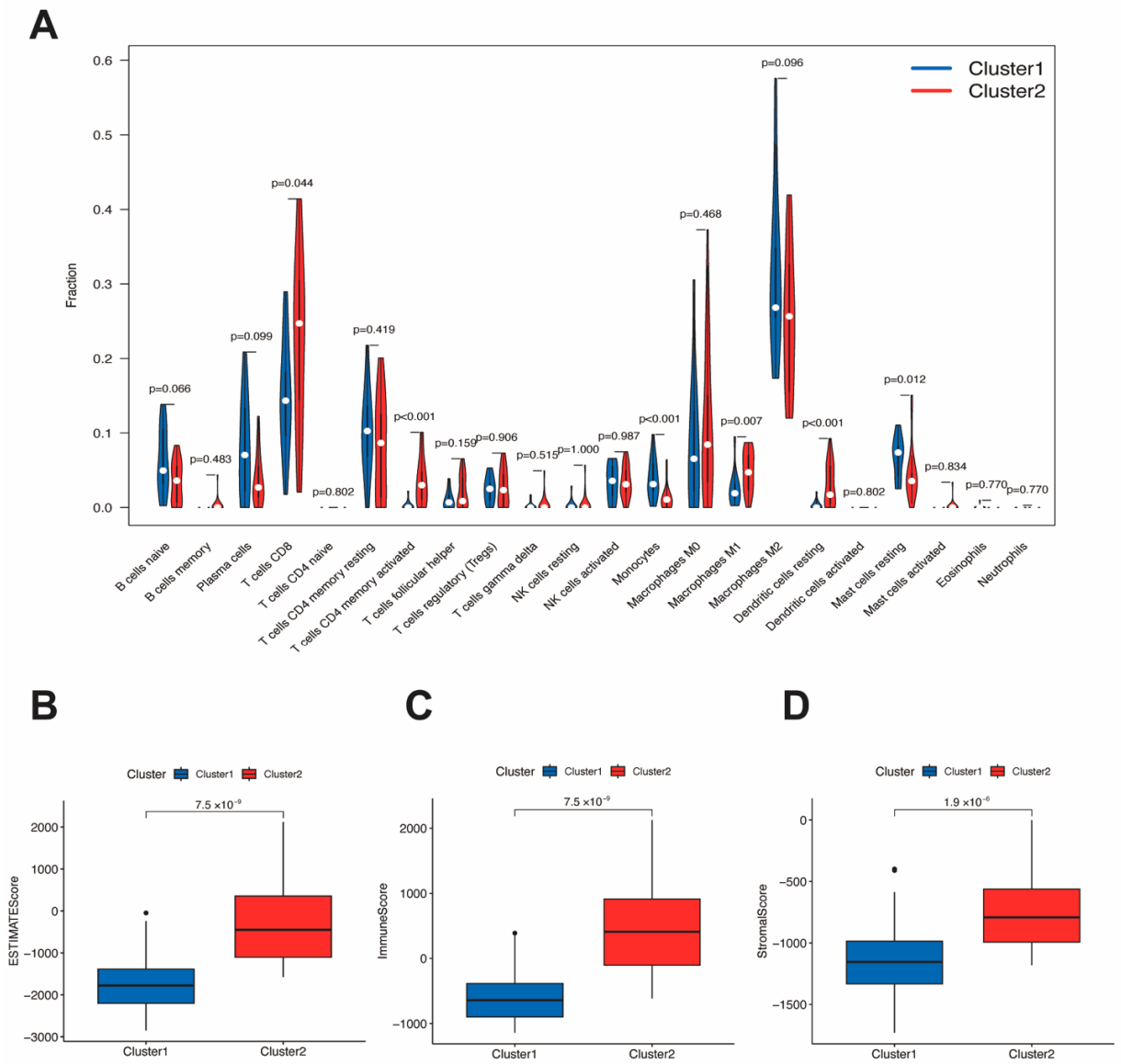


**Figure 5: Correction between subtypes and level of immune cell infiltration in the TIME.** (**A**) The fraction of different immune cells in cluster1 and cluster2. (**B–D**): Difference of ESTIMATEScore, immuneScore and StronalScore in two clusters.

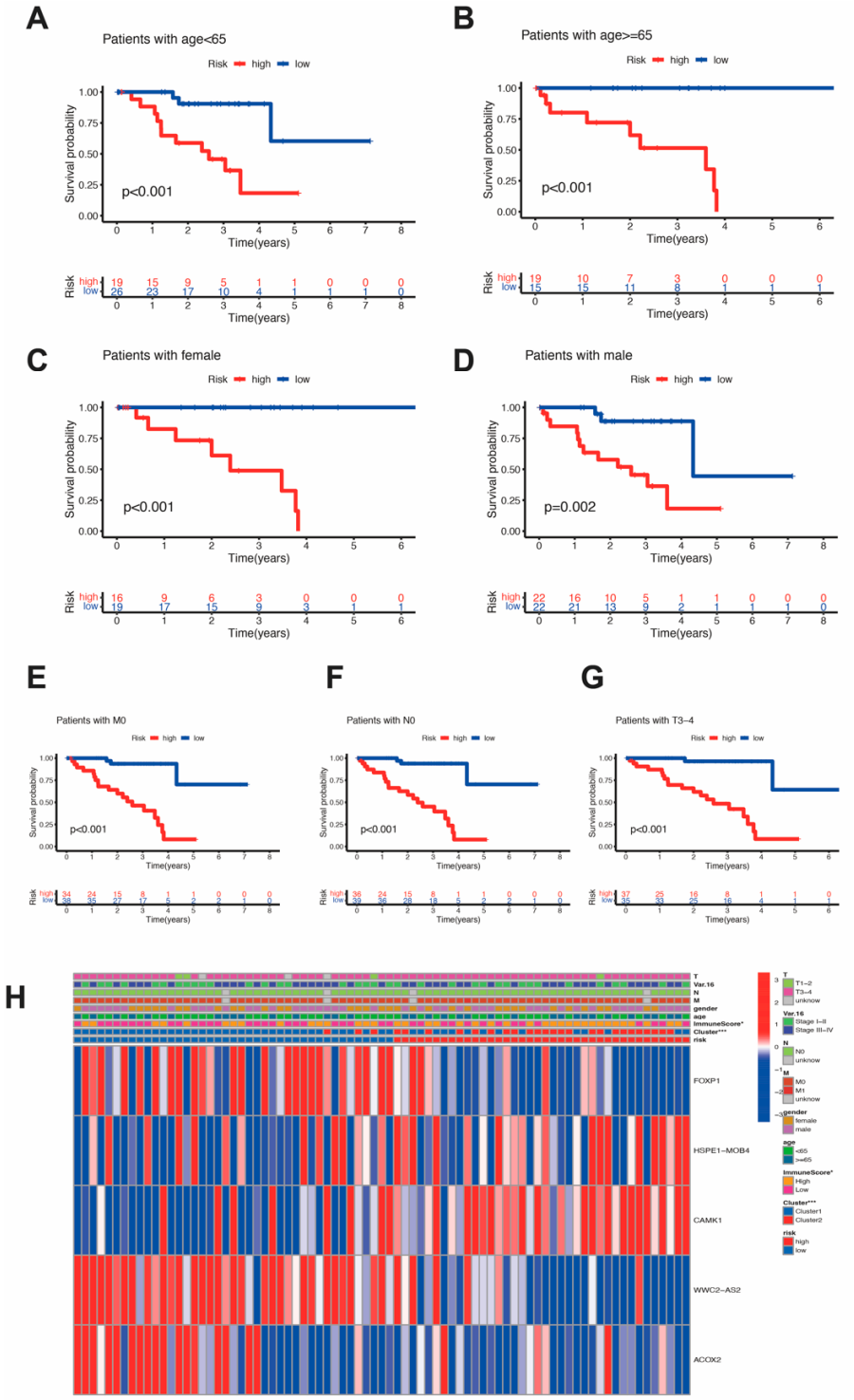


**Figure 6: Relationship between the OS and clinical features.** (**A–G**) Relationship between the OS and age, gender, M stage, N stage and T stage. (**H**) Different expression of prognostic genes in different clusters and above clinical features.

2024, Vol. 1, Article ID. 2024.0005
www.doi.org/10.69709/GenomC.2024.196011

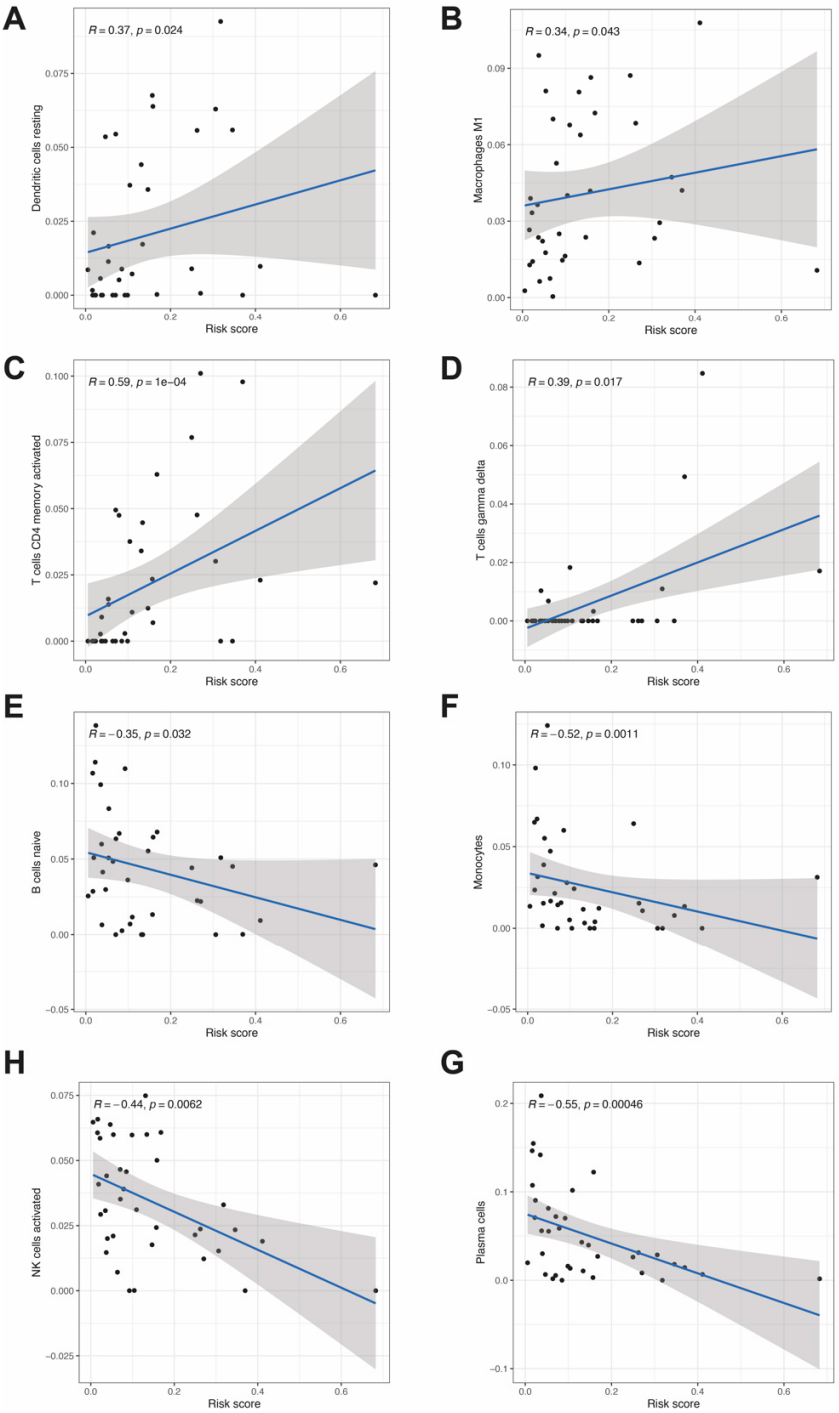


**Figure 7: Relationships between the risk score and infiltration abundances of immune cell types.** (**A**–**D**). Positive correction between risk score and the fraction of immune cells in Tumor Immune Microenvironment (TIME). (**E**–**H**). Negative relationship with risk score and the fraction of immune cells.

ing and promote degradation of faulty proteins [25]. Research reports show that compared to non-cancer bladder epithelial cells, the level of HSPE1 in tumor cells is significantly higher, suggesting that *HSPE1* may be an effective tumor tissue biomarker for specific detection of bladder cancer [26]. Murine human like alpha-chemokine analog one binder family member 4 (*MOB4*), is a member of the MOB family that can bind to protein kinases and play a role in the transduction of auxiliary signals in the cell [27]. A study by analysis of pan-cancer showed that MOB4 can bind to PDCD10 (programmed cell death 10) and be involved in the development of different tumors through the Hippo signaling pathway, RNA transport, mRNA surveillance pathway, internalization process, and T cell receptor signaling pathway [28].

In this study, altered gene expression profiles were identified that may be linked to the activation of these pathways. Specifically, the differential expression of key genes in the mTOR and P53 pathways, particularly those with high hazard ratios such as *HSPE1-MOB4*, *HLA-DRB1*, and *CAMK1*, could be influenced by the hyperactivation of the MAPK/YAP pathways due to GNAQ/GNA11 mutations. These mutations likely contribute to the altered transcriptional landscape we observed, promoting aggressive tumor phenotypes and poor survival outcomes in cluster 2 UVM patients. Furthermore, while the GNAQ and GNA11 mutations themselves do not directly correlate with changes in RNA expression levels, they induce downstream effects that lead to aberrant transcriptional activity. For example, genes involved in the immune microenvironment and tumor invasion, such as *HLA-DRB1*, are upregulated, potentially as a result of the signaling cascades initiated by these mutations [2,8,9].

It was indicated in the study that prognostic RNA in Uveal melanoma (UM) mainly focus on the P53 and mTOR pathway. Previous researches have showed that these two pathways are enriched in various cancer types, such as breast cancer, bladder cancer, lung cancer, and so on [29–32]. In particular, the P53 pathway has been considered to be essential for tumor suppression, and thus, has been utilized for gene therapy, which had met success in treating non-small cell lung carcinoma (NSCLC) patients, both in the USA and China [33,34]. This method could be considered as a potential treatment for UM in the future. Apart from that, mTOR is one of the most frequently mutated or altered pathways in tumors, which plays a crucial role in regulating cell proliferation, growth, differentiation and survival. Several clinical treatments, such as rapamycin therapy, have been developed to suppress the mTOR pathway [35–37]. Therefore, it is worth exploring whether this method can be used to treat Uveal melanoma.

Apart from that, 5 prognostic RNA was identified to build the risk model and these expressions could be very useful indicators to diagnose Uveal melanoma in the clinical. Using this equation, patients can be categorized into low-risk and high-risk groups, allowing for the prediction of their overall survival. Furthermore, it has been suggested that the fraction of six immune cell types has a positive or inverse correlation with the risk score. For instance, there is a positive correlation between risk score and fraction of Macrophages M1 and T cells in TIME, implying that these immune cells might promote the development and spread of uveal melanoma. Meanwhile, the four other cell types can act as suppressors of tumor development, like NK/B cells, monocytes cells and plasma cells. Research on the tumor immune environment of cancer has been conducted and major (immune)-therapeutic approaches targeting specific fractions of immune cells have been studied in ovarian, cervical and breast cancer [38–41]. Similarly, UM could potentially be treated by manipulating the fraction of immune cells; however, further investigation is needed.

## 5. Conclusions

After employing various bioinformatics techniques and statistical analyses, this study proposed that 32 genes significantly impact the prognosis of uveal melanoma (UM), which can be used to construct a risk model for predicting patients' survival time. Among them, *HSPE1-MOB4* demonstrated the highest risk ratio, thus potentially playing an essential role in predicting prognosis of patients with UM. Additionally, it was discovered that the fraction of certain immune cell types in TIME had either a positive or negative correlation with changes in the risk score. Moreover, two subtypes with significantly different survival rates have been identified, as well as distinct pathways associated with them. To gain further insights into the molecular mechanisms, more research will be necessary to validate the accuracy of our resulting analyses.

## Author Contributions

All authors contributed to the study conception and design. Data collection and analysis were performed by M.D., J.S. and Y.S. The first draft of the manuscript was written by Y.S. and all authors commented on previous versions of the manuscript. All authors have read and agreed to the published version of the manuscript.

## Data and Materials Availability Statement

The datasets presented in this study can be found in online repositories. The names of the repository/repositories and accession number(s) can be found below: https://tcga-data.nci.nih.gov/tcga/ (accessed on 5 March 2023), project TCGA-UVM.

## Consent for Publication

Not applicable.

## Conflicts of Interest

The authors declare that the research was conducted in the absence of any commercial or financial relationships that could be construed as a potential conflict of interest.

## Funding

This work was supported by the Natural Science Foundation of Shandong Province of China (ZR2020MH173).

## Acknowledgments

We thank all members of Eye center and Clinical Research Center for helpful discussion.

## Supplementary Materials

Download the Supplementary data to this article. Figure S1: Flowchart of the present study. Figure S2: The relationship between genes having significant expression related to prognosis and the overall survival (OS). Figure S3: Similarity analysis of RNAs expression levels and ambiguous clustering. Figure S4: Construction of the risk model about uveal melanoma. Figure S5: Correction between clusters and the fraction of immune cells. Figure S6: The relationship with clusters and risk score.

## Ethics Statement

Not applicable.

### References

[1] Carvajal, R.D.; Butler, M.O.; Shoushtari, A.N.; Hassel, J.C.; Ikeguchi, A.; Hernandez-Aya, L.; Nathan, P.; Hamid, O.; Piulats, J.M.; Rioth, M.; et al. Clinical and molecular response to tebentafusp in previously treated patients with metastatic uveal melanoma: a phase 2 trial. *Nat. Med.* **2022**, *28*, 2364–2373. [CrossRef] [PubMed]

[2] Smit, K.N.; Jager, M.J.; de Klein, A.; Kiliç , E. Uveal melanoma: towards a molecular understanding. *Prog. Retin. Eye Res.* **2020**, *75*, 100800. [CrossRef] [PubMed]

[3] Durante, M.A.; Rodriguez, D.A.; Kurtenbach, S.; Kuznetsov, J.N.; Sanchez, M.I.; Decatur, C.L.; Snyder, H.; Feun, L.G.; Livingstone, A.S.; Harbour, J.W. Single-cell analysis reveals new evolutionary complexity in uveal melanoma. *Nat. Commun.* **2020**, *11*, 496. [CrossRef] [PubMed]

[4] Rodriguez-Vidal, C.; Fernandez-Diaz, D.; Fernandez-Marta, B.; Lago-Baameiro, N.; Pardo, M.; Silva, P.; Paniagua, L.; Blanco-Teijeiro, M.J.; Piñeiro, A.; Bande, M. Treatment of metastatic uveal melanoma: systematic review. *Cancers* **2020**, *12*, 2557. [CrossRef]

[5] Schank, T.E.; Hassel, J.C. Immunotherapies for the treatment of uveal melanoma-history and future. *Cancers* **2019**, *11*, 1048. [CrossRef]

[6] Violanti, S.S.; Bononi, I.; Gallenga, C.E.; Martini, F.; Tognon, M.; Perri, P. New insights into molecular oncogenesis and therapy of uveal melanoma. *Cancers* **2019**, *11*, 694. [CrossRef]

[7] Johansson, P.A.; Brooks, K.; Newell, F.; Palmer, J.M.; Wilmott, J.S.; Pritchard, A.L.; Broit, N.; Wood, S.; Carlino, M.S.; Leonard, C.; et al. Whole genome landscapes of uveal melanoma show an ultraviolet radiation signature in iris tumours. *Nat. Commun.* **2020**, *11*, 2408. [CrossRef]

[8] Griewank, K.G.; Yu, X.; Khalili, J.; Sozen, M.M.; Stempke-Hale, K.; Bernatchez, C.; Wardell, S.; Bastian, B.C.; Woodman, S.E. Genetic and molecular characterization of uveal melanoma cell lines. *Pigment Cell Melanoma Res.* **2012**, *25*, 182–187. [CrossRef]

[9] Spagnolo, F.; Caltabiano, G.; Queirolo, P. Uveal melanoma. *Cancer Treat. Rev.* **2012**, *38*, 549–553. [CrossRef]

[10] Helgadottir, H.; Höiom, V. The genetics of uveal melanoma: current insights. *Appl. Clin. Genet.* **2016**, *9*, 147–155.

[11] Wilkerson, M.D.; Hayes, D.N. Consensusclusterplus: a class discovery tool with confidence assessments and item tracking. *Bioinformatics* **2010**, *26*, 1572–1573. [CrossRef] [PubMed]

[12] Yu, G.; Wang, L.G.; Han, Y.; He, Q.Y. Clusterprofiler: an R package for comparing biological themes among gene clusters. *OMICS* **2012**, *16*, 284–287. [CrossRef] [PubMed]

[13] Subramanian, A.; Tamayo, P.; Mootha, V.K.; Mukherjee, S.; Ebert, B.L.; Gillette, M.A.; Paulovich, A.; Pomeroy, S.L.; Golub, T.R.; Lander, E.S.; et al. Gene set enrichment analysis: a knowledge-based approach for interpreting genome-wide expression profiles. *Proc. Natl. Acad. Sci. USA* **2005**, *102*, 15545–15550. [CrossRef] [PubMed]

[14] Yoshihara, K.; Shahmoradgoli, M.; Martínez, E.; Vegesna, R.; Kim, H.; Torres-Garcia, W.; Treviño, V.; Shen, H.; Laird, P.W.; Levine, D.A.; et al. Inferring tumour purity and stromal and immune cell admixture from expression data. *Nat. Commun.* **2013**, *4*, 2612. [CrossRef] [PubMed]

[15] Chen, B.; Khodadoust, M.S.; Liu, C.L.; Newman, A.M.; Alizadeh, A.A. Profiling tumor infiltrating immune cells with CIBERSORT. *Methods Mol. Biol.* **2018**, *1711*, 243–259. [PubMed]

[16] Bøvelstad, H.M.; Nygård, S.; Størvold, H.L.; Aldrin, M.; Borgan, Ø.; Frigessi, A.; Lingjaerde, O.C. Predicting survival from microarray data--a compar-

ative study. *Bioinformatics* **2007**, *23*, 2080–2087. [CrossRef]

[17] Xu, F.; Zhan, X.; Zheng, X.; Xu, H.; Li, Y.; Huang, X.; Lin, L.; Chen, Y. A signature of immune-related gene pairs predicts oncologic outcomes and response to immunotherapy in lung adenocarcinoma. *Genomics* **2020**, *112*, 4675–4683. [CrossRef]

[18] Prensner, J.R.; Zhao, S.; Erho, N.; Schipper, M.; Iyer, M.K.; Dhanasekaran, S.M.; Magi-Galluzzi, C.; Mehra, R.; Sahu, A.; Siddiqui, J.; et al. RNA biomarkers associated with metastatic progression in prostate cancer: a multi-institutional high-throughput analysis of schlap1. *Lancet Oncol.* **2014**, *15*, 1469–1480. [CrossRef]

[19] Li, H.; Chen, L.; Han, Y.; Zhang, F.; Wang, Y.; Han, Y.; Wang, Y.; Wang, Q.; Guo, X. The identification of RNA modification gene pus7 as a potential biomarker of ovarian cancer. *Biology* **2021**, *10*, 1130. [CrossRef]

[20] Brase, J.C.; Schmidt, M.; Fischbach, T.; Sültmann, H.; Bojar, H.; Koelbl, H.; Hellwig, B.; Rahnenführer, J.; Hengstler, J.G.; Gehrmann, M.C. Erbb2 and top2A in breast cancer: a comprehensive analysis of gene amplification, RNA levels, and protein expression and their influence on prognosis and prediction. *Clin. Cancer Res.* **2010**, *16*, 2391–2401. [CrossRef]

[21] Lai, X.; Umbricht, C.B.; Fisher, K.; Bishop, J.; Shi, Q.; Chen, S. Identification of novel biomarker and therapeutic target candidates for diagnosis and treatment of follicular carcinoma. *J. Proteomics* **2017**, *166*, 59–67. [CrossRef] [PubMed]

[22] Nowell, P.C. The minute chromosome (phl) in chronic granulocytic leukemia. *Blut* **1962**, *8*, 65–66. [CrossRef] [PubMed]

[23] Rowley, J.D. Letter: A new consistent chromosomal abnormality in chronic myelogenous leukaemia identified by quinacrine fluorescence and giemsa staining. *Nature* **1973**, *243*, 290–293. [CrossRef]

[24] Rowley, J.D. Chromosomal translocations: revisited yet again. *Blood* **2008**, *112*, 2183–2189. [CrossRef] [PubMed]

[25] Macario, A.J.; Conway de Macario, E. Sick chaperones, cellular stress, and disease. *N. Engl. J. Med.* **2005**, *353*, 1489–1501. [CrossRef] [PubMed]

[26] Tsai, C.H.; Chen, Y.T.; Chang, Y.H.; Hsueh, C.; Liu, C.Y.; Chang, Y.S.; Chen, C.L.; Yu, J.S. Systematic verification of bladder cancer-associated tissue protein biomarker candidates in clinical urine specimens. *Oncotarget* **2018**, *9*, 30731–30747. [CrossRef]

[27] Gundogdu, R.; Hergovich, A. MOB (mps one binder) proteins in the hippo pathway and cancer. *Cells* **2019**, *8*, 569. [CrossRef]

[28] Sun, N.; Li, C.; Teng, Y.; Deng, Y.; Shi, L. Pan-cancer analysis on the oncogenic role of programmed cell death 10. *J. Oncol.* **2022**, *2022*, 1242658. [CrossRef]

[29] Borchers, A.; Pieler, T. Programming pluripotent precursor cells derived from xenopus embryos to generate specific tissues and organs. *Genes* **2010**, *1*, 413–426. [CrossRef]

[30] Puzio-Kuter, A.M.; Castillo-Martin, M.; Kinkade, C.W.; Wang, X.; Shen, T.H.; Matos, T.; Shen, M.M.; Cordon-Cardo, C.; Abate-Shen, C. Inactivation of p53 and pten promotes invasive bladder cancer. *Genes Dev.* **2009**, *23*, 675–680. [CrossRef]

[31] Liang, Z.; Zhong, Y.; Meng, L.; Chen, Y.; Liu, Y.; Wu, A.; Li, X.; Wang, M. Hax1 enhances the survival and metastasis of non-small cell lung cancer through the akt/mTOR and mdm2/p53 signaling pathway. *Thorac. Cancer* **2020**, *11*, 3155–3167. [CrossRef] [PubMed]

[32] Cai, J.; Xia, J.; Zou, J.; Wang, Q.; Ma, Q.; Sun, R.; Liao, H.; Xu, L.; Wang, D.; Guo, X. The pi3k/mTOR dual inhibitor nvp-bez235 stimulates mutant p53 degradation to exert anti-tumor effects on triple-negative breast cancer cells. *FEBS Open Bio* **2020**, *10*, 535–545. [CrossRef] [PubMed]

[33] Roth, J.A.; Nguyen, D.; Lawrence, D.D.; Kemp, B.L.; Carrasco, C.H.; Ferson, D.Z.; Hong, W.K.; Komaki, R.; Lee, J.J.; Nesbitt, J.C.; et al. Retrovirus-mediated wild-type p53 gene transfer to tumors of patients with lung cancer. *Nat. Med.* **1996**, *2*, 985–991. [CrossRef]

[34] Lane, D.P.; Cheok, C.F.; Lain, S. P53-based cancer therapy. *Cold. Spring Harb. Perspect. Biol.* **2010**, *2*, a001222. [CrossRef] [PubMed]

[35] Huang, S.; Houghton, P.J. Targeting mTOR signaling for cancer therapy. *Curr. Opin. Pharmacol.* **2003**, *3*, 371–377. [CrossRef]

[36] Tian, T.; Li, X.; Zhang, J. MTOR signaling in cancer and mTOR inhibitors in solid tumor targeting therapy. *Int. J. Mol. Sci.* **2019**, *20*, 755. [CrossRef]

[37] Easton, J.B.; Houghton, P.J. MTOR and cancer therapy. *Oncogene* **2006**, *25*, 6436–6446. [CrossRef]

[38] Baci, D.; Bosi, A.; Gallazzi, M.; Rizzi, M.; Noonan, D.M.; Poggi, A.; Bruno, A.; Mortara, L. The ovarian cancer tumor immune microenvironment (time) as target for therapy: A focus on innate immunity cells as therapeutic effectors. *Int. J. Mol. Sci.* **2020**, *21*, 3125. [CrossRef]

[39] Yang, L.; Yang, Y.; Meng, M.; Wang, W.; He, S.; Zhao, Y.; Gao, H.; Tang, W.; Liu, S.; Lin, Z.; et al. Identification of prognosis-related genes in the cervical cancer immune microenvironment. *Gene* **2021**, *766*, 145119. [CrossRef]

[40] Chen, S.; Krinsky, A.L.; Woolaver, R.A.; Wang, X.; Chen, Z.; Wang, J.H. Tumor immune microenvironment in head and neck cancers. *Mol. Carcinog.* **2020**, *59*, 766–774. [CrossRef]

[41] Xiong, Y.; Wang, Y.; Tiruthani, K. Tumor immune microenvironment and nano-immunotherapeutics in colorectal cancer. *Nanomedicine* **2019**, *21*, 102034. [CrossRef] [PubMed]